nature nanotechnology

LETTERS

PUBLISHED ONLINE: 19 DECEMBER 2010 | DOI: 10.1038/NNANO.2010.250

Nanoparticle-induced unfolding of fibrinogen promotes Mac-1 receptor activation and inflammation

Zhou J. Deng[1], Mingtao Liang[2,3], Michael Monteiro[4], Istvan Toth[2,3] and Rodney F. Minchin[1]*

The chemical composition, size, shape and surface characteristics of nanoparticles affect the way proteins bind to these particles, and this in turn influences the way in which nanoparticles interact with cells and tissues[1–5]. Nanomaterials bound with proteins can result in physiological and pathological changes, including macrophage uptake[1,6], blood coagulation[7], protein aggregation[8] and complement activation[7,9], but the mechanisms that lead to these changes remain poorly understood. Here, we show that negatively charged poly(acrylic acid)-conjugated gold nanoparticles bind to and induce unfolding of fibrinogen, which promotes interaction with the integrin receptor, Mac-1. Activation of this receptor increases the NF-κB signalling pathway, resulting in the release of inflammatory cytokines. However, not all nanoparticles that bind to fibrinogen demonstrated this effect. Our results show that the binding of certain nanoparticles to fibrinogen in plasma offers an alternative mechanism to the more commonly described role of oxidative stress in the inflammatory response to nanomaterials.

Poly(acrylic acid)-coated gold nanoparticles (PAA–GNP)[10] with hydrodynamic diameters of ~5, 10 and 20 nm were first synthesized. Their interactions with human plasma proteins were then examined using one- and two-dimensional gel electrophoresis (Fig. 1). The negatively charged PAA coat prevented agglomeration in solution (Supplementary Fig. S1a). Nanoparticle–protein binding reached equilibrium within 5 min and remained constant over 4 h (Supplementary Fig. S1b). Moreover, bound proteins remained associated with the nanoparticles even after extensive washings, indicating a high-affinity interaction (Supplementary Fig. S1c). Sodium dodecylsulphate–polyacrylamide gel electrophoresis (SDS–PAGE) of human plasma proteins bound to PAA–GNP at equilibrium showed three major protein bands with molecular weights of ~65, 55 and 45 kDa (Fig. 1a). Two-dimensional gel electrophoresis (Supplementary Fig. S1d) and mass spectroscopy (Supplementary Table S1) confirmed that the three bands were α, β and γ chains of fibrinogen, respectively.

The binding capacity of the nanoparticles for the purified human fibrinogen was determined by ultracentrifugation (Fig. 1b). Consistent with Fig. 1a, the 20 nm PAA–GNP bound significantly less fibrinogen than the 5 nm particles on a mass basis. However, when adjusted for total surface area, the binding was found to be similar (Fig. 1b, inset). The maximum protein binding was 2 μg for the 5 nm PAA–GNP, which represents one to two nanoparticles per fibrinogen molecule (nanoparticle density, 19.3 g cm^{-3}; diameter, 5.0–5.5 nm). For the 20 nm PAA–GNP, maximum binding was 8 μg nanoparticles, or approximately seven molecules of fibrinogen per nanoparticle. This variance was probably due to differences in surface area (78 nm^2 and 1,040 nm^2 for the 5 and 20 nm PAA–GNP, respectively), suggesting the configuration of bound fibrinogen may vary for each nanoparticle.

Fibrinogen[11], which has a length of ~45 nm and diameter of 5 nm, is much larger than the 5 nm PAA–GNP. The low stoichiometry therefore suggests that the nanoparticles interact with specific sites on the protein. Fibrinogen comprises three protein chains (α, β and γ) arranged as a dimer, with three domains: a central E domain with two peripheral D domains[11] (Fig. 1c). The protein is negatively charged at physiological pH (pI = 5.5), so its high-affinity interaction with the negatively charged 5 nm PAA–GNP was unexpected. The C-terminus of each α chain may act as a potential binding site[12], as it is positively charged at pH 7.4. Other than its role in clotting, fibrinogen also binds to surfaces, unfolding to expose sequences normally embedded within the protein[13]. One sequence, amino acids 377–395 in the C-terminus of the γ chain ($\gamma^{377-395}$), is located in the D domain and is responsible for the recruitment of macrophages and leukocytes (Fig. 1c, inset). This is achieved by the interaction of $\gamma^{377-395}$ with the Mac-1 receptor (CD11b/CD18 or $\alpha_M\beta_2$)[13]. The positively charged C-terminus of the α chain is located adjacent to the D domain. We therefore posed the question of whether PAA–GNP could induce unfolding of the fibrinogen molecule and Mac-1 receptor binding.

Far-ultraviolet circular dichroism was first used to monitor the protein structure in the presence of increasing amounts of 5 nm PAA–GNP. The spectrum for fibrinogen alone was typical for a protein with both α-helix and β-sheet structure (Fig. 1d). The addition of PAA–GNP resulted in a loss of protein secondary structure, as indicated by the progressive increase in ellipticity. Based on these observations, we surmised that the PAA–GNP induces changes in the fibrinogen structure that may expose the γC-terminus, similar to previous reports for flat surfaces[13]. Figure 2a shows that the 5 nm PAA–GNP significantly increased the binding of fibrinogen to Mac-1-receptor-positive THP-1 cells but not to Mac-1-receptor-negative HL-60 cells, an effect not seen with albumin. To further establish binding specificity, Mac-1-receptor-negative HEK293 cells were transfected with CD11b and CD18 (Fig. 2b, upper panel). In empty vector-transfected cells, no change in fibrinogen binding was seen in the presence of PAA–GNP, but it increased more than twofold in the CD11b/CD18-transfected cells (Fig. 2b). These experiments show that fibrinogen bound to 5 nm PAA–GNP interacts with the Mac-1 receptor. However, the larger nanoparticles (20 nm) did not promote cell interaction to the same extent when adjusted for similar protein binding (Fig. 2c).

[1]School of Biomedical Sciences, University of Queensland, Brisbane 4072, Australia, [2]School of Chemistry and Molecular Biosciences, University of Queensland, Brisbane 4072, Australia, [3]School of Pharmacy, University of Queensland, Brisbane 4072, Australia, [4]Australian Institute for Bioengineering and Nanotechnology, University of Queensland, Brisbane 4072, Australia. *e-mail: r.minchin@uq.edu.au

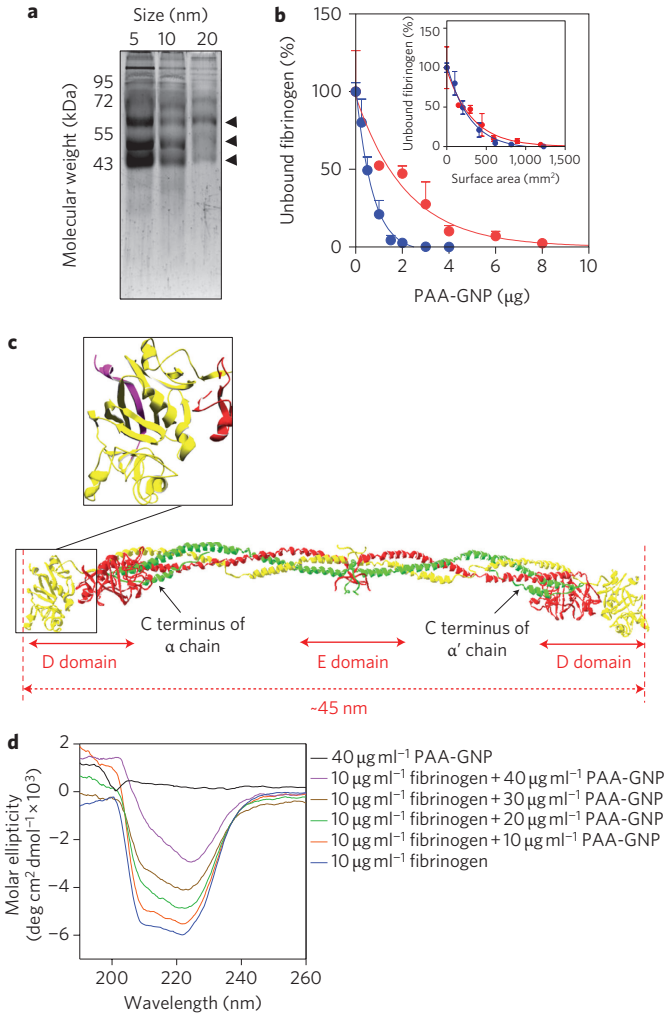

Figure 1 | Fibrinogen is the major human plasma protein bound by PAA–GNP. a, SDS–PAGE of human plasma proteins bound to PAA–GNP with diameters of 5, 10 and 20 nm. Three major protein bands were observed at ~65, 55 and 45 kDa. **b**, Unbound fibrinogen following pull-down with PAA–GNP with diameters of ~5 nm (blue) or 20 nm (red). Purified fibrinogen (0.6 μg) was incubated with increasing amounts of PAA–GNP. Inset: unbound fibrinogen is plotted against total surface area for the two nanoparticles. **c**, Crystal structure of fibrinogen. The protein was drawn using Swiss-PdbViewer and coordinates for PDB entry 3GHG. Common domains are shown. Inset: the C-terminus of the γ chain (purple) that interacts with the Mac-1 receptor. **d**, Circular dichroism of fibrinogen in the absence and presence of increasing concentrations of 5 nm PAA–GNP.

The peptide $\gamma^{377-395}$ (P2 = γ^{377}YSMKKTTMKIIPFNRLTIG^{395}) has been shown to inhibit Mac-1-mediated cell adhesion to immobilized fibrinogen[14]. We used P2 together with a control sequence (H19 = γ^{340}HAGHLNGVYYQ GGTYSKA^{357})[15] to further investigate nanoparticle-induced fibrinogen binding to the THP-1 cells. At concentrations as low as 10 μM, P2 significantly inhibited binding, but H19 had no effect (Fig. 2d). This result supports the model of nanoparticle-induced unfolding of the D-domain of fibrinogen. However, the 20 nm nanoparticles did not appear to expose the C-terminus of the γ chain. This was not due to a lack of protein unfolding, as demonstrated by circular dichroism (Supplementary Fig. S2). The apparent size of the 20 nm PAA–GNP in the presence of saturating fibrinogen, determined by dynamic light scattering, was 34.3 ± 0.6 nm ($n = 5$), suggesting that the fibrinogen corona extended ~7 nm from the nanoparticle surface. With each nanoparticle binding ~7 molecules of fibrinogen, crowding of the particle surface may result in steric hindrance, preventing the exposed C-terminus of the γ chain from interacting with the Mac-1 receptor. To address this, 20 nm PAA–GNPs were bound to decreasing amounts of fibrinogen (33–100% saturation) and incubated with THP-1 or HL-60 cells (Fig. 2e). Binding to THP-1 cells increased by more than a factor of six, but no change was seen with HL-60 cells, suggesting that steric hindrance prevented Mac-1 receptor interaction at high protein binding.

Mac-1 receptor activation increases NF-κB activity by promoting the degradation of IκB, which then allows NF-κB to translocate into the nucleus, and upregulates a number of pro-inflammatory genes[16]. To examine this, electromobility shift assays were performed using an NF-κB probe[17]. Fibrinogen bound to the 5 nm PAA–GNP increased nuclear NF-κB (Fig. 2f, lane 4), which was confirmed by anti-P65 antibody supershift (Fig. 2f, lane5). Fibrinogen (Fig. 2f, lane 2) and PAA–GNP alone (Fig. 2f, lane 3) also increased NF-κB in the nucleus, albeit to a lower extent. Soluble fibrinogen is known to activate NF-κB in several cell lines[18] via receptors other than Mac-1. These results show that the fibrinogen/PAA–GNP complexes can increase nuclear NF-κB in THP-1 cells.

NF-κB has been implicated as a key factor in many inflammatory diseases[19]. To test whether fibrinogen bound to PAA–GNP could increase secretion of inflammatory cytokines, THP-1 cells were treated with either fibrinogen or 5 nm PAA–GNP, or both (Fig. 3a,b). Neither fibrinogen nor PAA–GNP alone altered cytokine release, but the fibrinogen/PAA–GNP complex increased IL-8 and TNF-α secretion by factors of 28 and 67, respectively (Fig. 3a,b). This increase was attenuated by BAY 11-7082, an inhibitor of the NF-κB pathway. Cells treated with fibrinogen and the 20 nm PAA–GNP secreted cytokine only when non-saturating protein levels were used (Fig. 3c–f). This is consistent with the results shown in Fig. 2e.

We next investigated whether the surface charge density of the 5 nm PAA–GNPs was affecting fibrinogen binding, by using increasing proportions of the neutral polymer poly(2,3-hydroxy-propylacrylamide) (PDHA) in the polymer coating (Supplementary Table S2), which progressively increased the zeta potential (Supplementary Fig. S3). Fibrinogen binding decreased significantly with 20% PDHA, and was completely inhibited at higher proportions of PDHA (Fig. 4a). Fibrinogen did not bind to THP-1 cells in the presence of any PDHA-containing nanoparticles (Fig. 4b). These results show that surface charge density is a critical factor for fibrinogen binding and that small changes in charge density can influence the ability of the fibrinogen–nanoparticle complexes to interact with the Mac-1 receptor.

Previously, metal-oxide nanoparticles have been shown to bind an array of plasma proteins including fibrinogen[5]. In this experiment, nano-SiO_2 (7 nm), nano-TiO_2 (21 nm) and nano-ZnO (30 nm) bound fibrinogen with approximately equal capacities (Fig. 4c). However, their ability to promote fibrinogen binding to THP-1 cells varied markedly. The smallest metal oxide (nano-SiO_2) increased fibrinogen binding by more than a factor of 20, whereas the largest metal oxide (nano-ZnO) showed no significant binding (Fig. 4d). Moreover, binding of nano-SiO_2–fibrinogen to THP-1 cells was inhibited by P2 (Fig. 4e) indicating that at least part of the cell interaction involved Mac-1. These results suggest that binding to fibrinogen alone does not predict Mac-1 receptor interaction.

A number of studies have shown that nanoparticle-bound proteins undergo conformational changes[20–22] and it has been suggested that unfolding of proteins could trigger the immune system by exposing normally buried sequences[3,4]. It has been shown that a high-affinity Mac-1 binding site exists in the γC-terminal tail region of fibrinogen. However, it is normally buried and protected within the hydrophobic core of the protein[15]. This

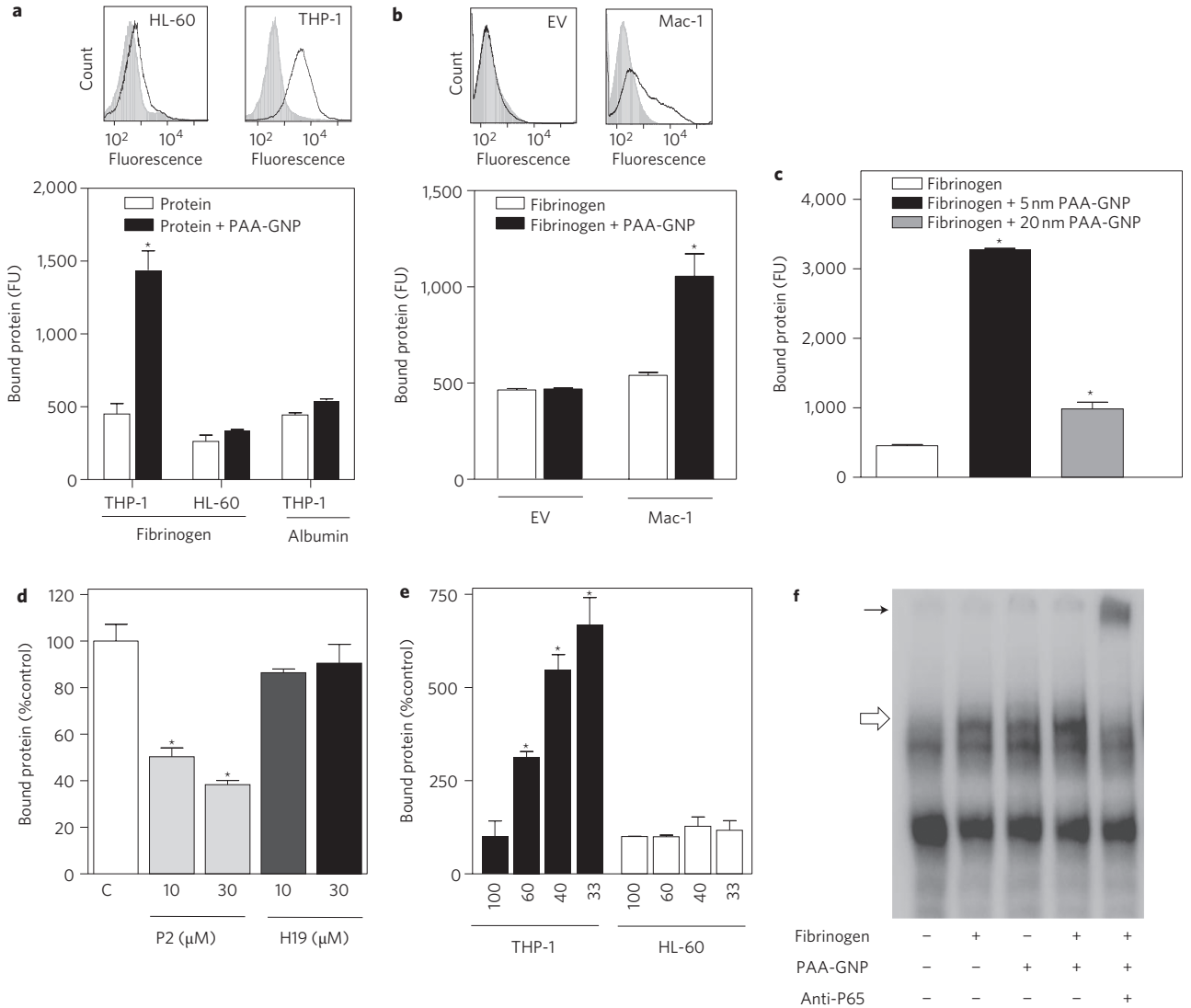

Figure 2 | Selective binding of fibrinogen/PAA-GNP complexes to Mac-1 receptors. a, HL-60 cells are Mac-1-receptor-negative cells, as shown by flow cytometry following labelling with fluorescent CD11b antibodies (upper panel, solid lines) and THP-1 cells are Mac-1-receptor-positive. This was confirmed by plating both HL-60 and THP-1 cells onto immobilized fibrinogen (Supplementary Fig. S4). Lower panel shows binding of fibrinogen alone (open bars) or fibrinogen with 5 nm PAA-GNP (filled bars) to THP-1 cells and HL-60 is shown. Addition of nanoparticles significantly increased the binding to THP-1 cells but not to HL-60 cells. Replacing fibrinogen with albumin abrogated the effect of the nanoparticles. Results are mean ± s.e.m, $n = 3$; asterisk indicates $P < 0.05$. **b**, HEK293 cells were transfected with empty vector (EV) or CD11b/CD18 constructs and Mac-1 receptor expression was determined by flow cytometry (upper panels). Lower panel shows binding of fibrinogen alone (open bars) or fibrinogen with 5 nm PAA-GNP (filled bars) is shown. The nanoparticles increased fibrinogen binding in Mac-1-receptor-positive cells only. Results are mean ± s.e.m., $n = 3$; asterisk indicates $P < 0.05$. **c**, PAA-GNP (20 nm) did not induce fibrinogen binding to THP-1 cells to the same extent as the 5 nm. Binding was performed with an equal surface area (3,900 mm^2) for each of the nanoparticles to ensure similar protein binding. **d**, Pre-treatment of THP-1 cells with the P2 peptide significantly reduced the binding of fibrinogen in the presence of 5 nm PAA-GNP (grey bars). Control peptide, H19, showed no inhibitory effects on binding (filled bars). Results are mean ± s.e.m., $n = 3$. **e**, PAA-GNP (20 nm) induced fibrinogen binding to THP-1 cells when the level of protein binding was reduced. However, no increase in binding was seen under the same conditions in HL-60 cells. Percent binding saturation is shown on the *x*-axis and was determined from the data shown in Fig. 1b. Results are mean ± s.e.m., $n = 3$, expressed as a percentage of the control (100%). **f**, Electrophoretic mobility shift assay, showing the increased nuclear localization of NF-κB in THP-1 cells when exposed to the fibrinogen/PAA-GNP complexes. The open arrow indicates the location of the P65 complex of NF-κB, which was confirmed by a supershift (solid arrow) with anti-P65 antibody (lane 5).

strongly agrees with our observations that fibrinogen unfolds on nanoparticles, and nanoparticle-bound fibrinogen interacts with Mac-1 receptors. However, mere binding to fibrinogen does not predict Mac-1 receptor interaction. For particles as large as 20 nm, the degree of fibrinogen binding appears to influence the accessibility of the C-terminus of the γ chain. When completely bound by fibrinogen, the 20 nm PAA–GNP did not induce cytokine release. This is relevant to particles in the circulation where excess fibrinogen is available, and may be important in designing negatively charged nanoparticles for therapeutic use, such as drug delivery[23]. Interestingly, the nano-metal oxides also demonstrated size-dependent effects with fibrinogen. The metal oxides tend to agglomerate in physiological solution, resulting in irregularly shaped structures, often with single nanoparticles protruding from their surfaces[5]. This may provide sufficient surface curvature for the nano-SiO_2 to bind and unfold fibrinogen.

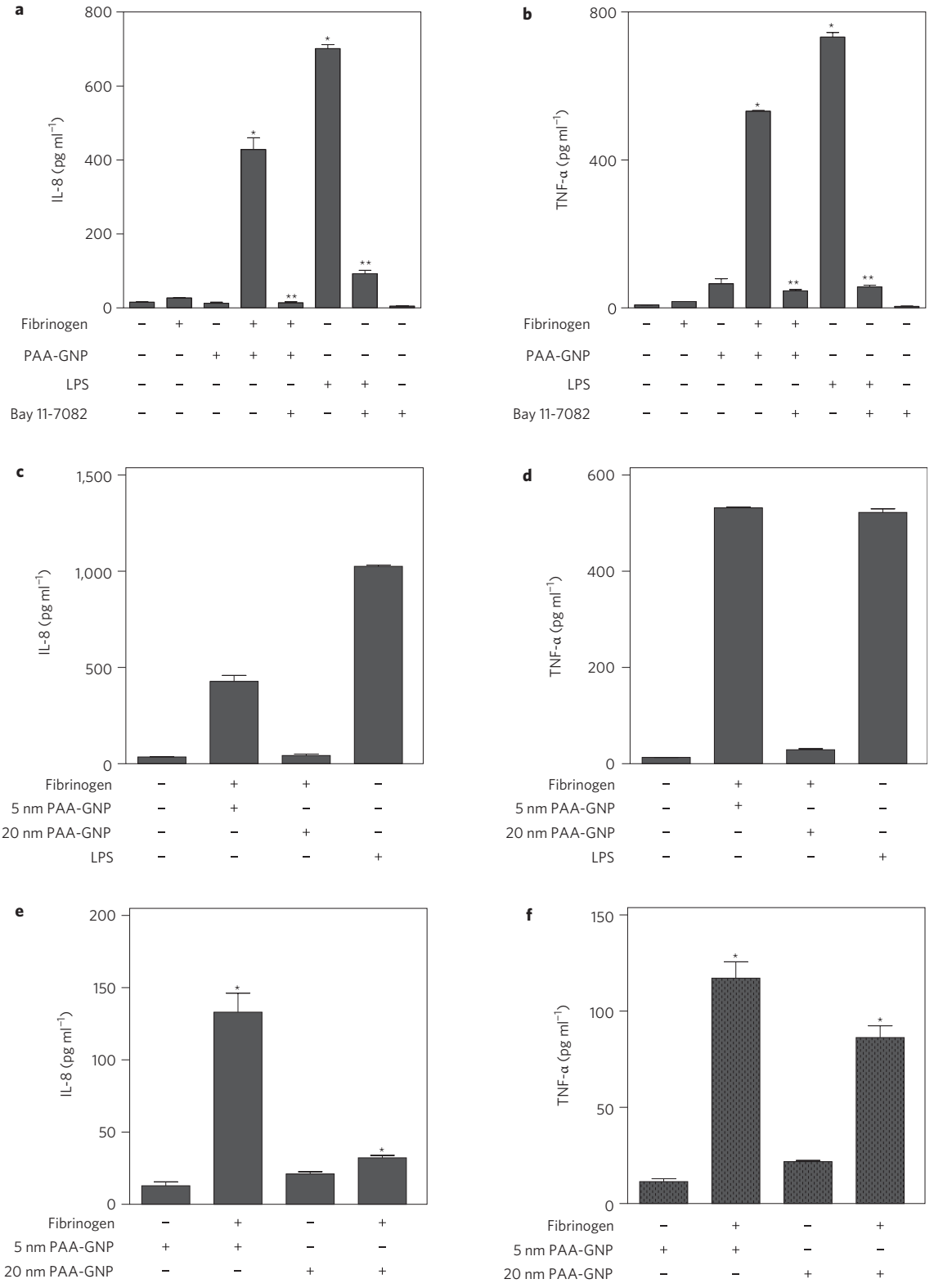

Figure 3 | Pro-inflammatory effects of fibrinogen/PAA-GNP complexes. a,**b**, Treatment of THP-1 cells with complexes of fibrinogen (33 μg ml^{-1}) and 5 nm PAA-GNP (100 μg ml^{-1}) induced the secretion of IL-8 (**a**) and TNF-α (**b**). Neither fibrinogen alone nor PAA-GNP altered cytokine release. The concentration effect of the complexes on cytokine release is shown in Supplementary Fig. S5. NF-κB pathway inhibitor, Bay 11-7082, inhibited the secretion of both cytokines. Lipopolysaccharide-treated cells were used as a positive control. Results are mean ± s.e.m., $n = 3$. Single asterisk indicates $P < 0.05$ compared to control (no treatment). Double asterisk indicates $P < 0.05$ compared to respective treatments without Bay 11-7082. **c**,**d**, THP-1 cells treated with 20 nm PAA-GNP bound to excess fibrinogen did not induce IL-8 (**c**) or TNF-α (**d**) release. Nanoparticles were adjusted to equal total surface area for similar protein binding. **e**,**f**, Cells treated with 20 nm PAA-GNP bound to a reduced concentration of fibrinogen (10 μg ml^{-1}), which resulted in only 33% binding saturation, induced low but significant release of IL-8 (**e**) and a more substantial release of TNF-α (**f**). Nanoparticles (5 nm; 30 μg ml^{-1}) bound to 10 μg ml^{-1} fibrinogen are shown for comparison. Asterisk indicates $P < 0.05$ compared to nanoparticles alone (respective controls).

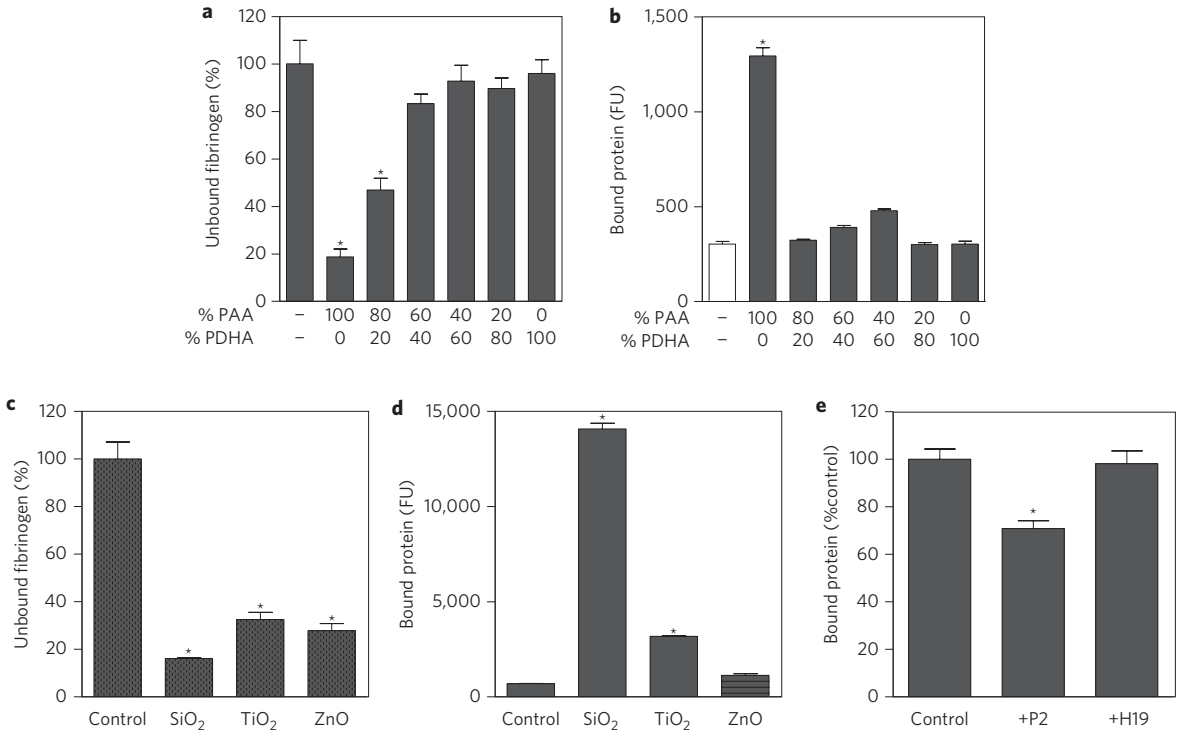

Figure 4 | Effects of nanoparticle surface characteristics on fibrinogen binding. a, Unbound fibrinogen following pull-down with PAA–PDHA–GNP. Purified fibrinogen (0.6 μg) was incubated with 2 μg of each nanoparticle. Only the 100% PAA/0% PDHA–GNP and 80% PAA/20% PDHA–GNP significantly bound fibrinogen. **b**, Binding of fibrinogen to THP-1 cells was only significantly increased with the nanoparticles containing 100% PAA. Results are mean ± s.e.m., $n = 3$. Asterisk indicates $P < 0.05$ compared to control (no treatment). **c**, Binding of fibrinogen to nano-metal oxides was determined by ultracentrifugation after mixing 0.6 μg protein with 8 μg nanoparticles. All the metal-oxide nanoparticles bound more than 70% of the fibrinogen. **d**, Binding of the fibrinogen–metal oxide complexes to THP-1 cells was determined. Results are mean ± s.e.m., $n = 3$. Asterisk indicates $P < 0.05$ compared to control (no treatment). **e**, Pre-treatment of THP-1 cells with the P2 peptide significantly reduced ($P < 0.05$) the binding of fibrinogen in the presence of nano-SiO_2. Control peptide, H19, showed no inhibitory effect on the binding. Results are mean ± s.e.m., $n = 3$.

The pro-inflammatory properties of different nanomaterials have been reported previously, often linked with the ability to induce oxidative stress[24–26]. However, recent studies suggest there is not always a good correlation between free radical generation and inflammation[27,28]. The current study proposes an alternative pathway for nanoparticles to provoke an inflammation response. Intriguingly, the interaction of fibrinogen and Mac-1 is critical for host immunity[29], and can exacerbate inflammation in conditions such as Alzheimer's[30] and arthritis[29]. Whether fibrinogen–nanoparticle complexes could aggravate those pathologies remains to be determined.

In summary, the current study shows that negatively charged nanoparticles can unfold fibrinogen and promote activation of the Mac-1 receptor pathway. As fibrinogen has been reported to bind many different types of nanomaterials in plasma, we propose that fibrinogen-bound nanoparticles are potentially pro-inflammatory.

Methods

Gold nanoparticles. PAA- and PDHA-coated spherical gold nanoparticles were synthesized and characterized as reported elsewhere[10]. The sources and characterization of the SiO_2 nanoparticles (nano-SiO_2), TiO_2 nanoparticles (nano-TiO_2) and ZnO nanoparticles (nano-ZnO) have been reported elsewhere[5].

Plasma protein binding. Human plasma samples were obtained from citrated blood of eight healthy individuals according to institutional bioethics approval. Nanoparticles in phosphate-buffered saline (150 mM sodium chloride and 10 mM phosphate, pH 7.4, PBS) were incubated with 1% human plasma at 37 °C for 5 min to 4 h and then separated from unbound proteins by centrifugation at 4 °C for 40 min (5 nm nanoparticles 50,000*g*; 10 nm nanoparticles 35,000*g*; 20 nm nanoparticles 20,000*g*). Plasma without nanoparticles was used as a control. Pellets were washed three times with PBS and reconstituted in SDS-containing buffer (1 mg ml^{-1} nanoparticles, 2% SDS, 5% β-mercaptoethanol, 10% glycerol and 62.5 mM Tris-HCl), heated at 95 °C for 5 min (ref. 5) and then separated by gel electrophoresis.

Protein separation and identification. Gel electrophoresis and mass spectrometry were performed as described previously[5]. (Running conditions, protein digestion and analysis procedures are provided in the Supplementary Information.)

Circular dichroism spectroscopy. Spectra were recorded using a J-815 circular dichroism spectrometer (JASCO) using a 10-mm path length quartz cell over the range 190–260 nm at ambient temperature. Data were collected every 0.2 nm with a bandwidth of 1 nm, at 50 nm min^{-1} and averaging over eight scans. Protein samples in PBS (10 μg ml^{-1}) were incubated with PAA–GNP for 5 min at ambient temperature before each measurement. The final spectra were baseline-corrected and data presented as mean residue ellipiticity (θ).

Protein labelling. Alexa Fluor 647 succinimidyl ester (Invitrogen) reconstituted in dimethylsulphoxide (125 μg ml^{-1}) was used to fluorescently label protein (2.5 mg ml^{-1}) in 150 mM sodium bicarbonate, pH 8.5 for 1 h. Free dye was removed using PD-10 desalting columns (GE Health). The far-red fluorescent dye was chosen to minimize interference from the PAA–GNP. The samples were stored in aliquots at −20 °C.

Cultured cell experiments. HL-60, HEK293 and THP-1 were obtained from the American Type Culture Collection (Manassas). Cells were cultured in RPMI 1640 with 5% fetal bovine serum and penicillin/streptomycin at 37 °C in 5% CO_2 in air. For protein binding studies, cells (5×10^5 per ml) were resuspended in the RPMI 1640 and incubated with 2.5 μg ml^{-1} fluorescently labelled protein in the presence or absence of 10 μg ml^{-1} nanoparticles for 20 min at 37 °C unless otherwise specified. For binding inhibition, cells were pre-treated with P2 or H19 peptides for 20 min at 37 °C. Following each binding study, cells were washed with RPMI 1640 and analysed by flow cytometry (BD FACSCanto, Becton Dickinson).

For transient transfection studies, HEK293 cells were seeded into six-well plates (1×10^6 per well) for 24 h, then transfected with 2.5 μg each of CD11b and CD18 plasmids (courtesy Dr E. Plow, Cleveland Clinic Foundation) using Lipofectamine™ 2000 (Invitrogen) according to the manufacturer's protocol. Cells were harvested 48 h later in 2 mM ethylenediaminetetraacetic acid and

resuspended in RPMI 1640. Receptor expression was assessed by flow cytometry after labelling cells with anti-CD11b antibody (ICRF44, Abcam) and Alexa Fluor 488-conjugated goat anti-mouse secondary antibody (Invitrogen). Mouse immunoglobulins were used as an isotype control.

For cytokine determination, cells (1×10^6 per ml) in the RPMI 1640 were treated with fibrinogen/PAA–GNP complexes (33 μg ml^{-1} and 100 μg ml^{-1}, respectively, unless otherwise specified) for 2 h at 37 °C. Cells alone and cells treated with either fibrinogen or nanoparticles were used as controls. All experiments were performed in polypropylene tubes to minimize surface adsorption of fibrinogen. After incubation, supernatants were harvested by centrifugation and cytokines were determined using a cytometric bead array kit (Becton Dickinson) according to the manufacturer's instruction. For NF-κB inhibition, cells were pre-treated with 30 μM Bay 11-7082 for 20 min at 37 °C before treatments.

Nuclear extraction and electrophoretic mobility shift assay (EMSA). Extraction of THP-1 cell nuclei and procedures for electrophoretic mobility shift assays have been described elsewhere[31]. Further details are provided in the Supplementary Information.

Statistical analysis. All experiments were performed at least three times. Data are presented as mean ± s.e.m. Statistical comparisons between different treatments were assessed by two-tailed *t* tests or one-way ANOVA assuming significance at $P < 0.05$.

Received 23 September 2010; accepted 16 November 2010; published online 19 December 2010

References

1. Ehrenberg, M. S., Friedman, A. E., Finkelstein, J. N., Oberdorster, G. & McGrath, J. L. The influence of protein adsorption on nanoparticle association with cultured endothelial cells. *Biomaterials* **30,** 603–610 (2009).
2. Fischer, H. C. & Chan, W. C. Nanotoxicity: the growing need for *in vivo* study. *Curr. Opin. Biotechnol.* **18,** 565–571 (2007).
3. Lynch, I. & Dawson, K. A. Protein–nanoparticle interactions. *Nano Today* **3,** 40–47 (2008).
4. Lynch, I., Salvati, A. & Dawson, K. A. Protein–nanoparticle interactions: what does the cell see? *Nature Nanotech.* **4,** 546–547 (2009).
5. Deng, Z. J. *et al.* Differential plasma protein binding to metal oxide nanoparticles. *Nanotechnology* **20,** 455101 (2009).
6. Dutta, D. *et al.* Adsorbed proteins influence the biological activity and molecular targeting of nanomaterials. *Toxicol. Sci.* **100,** 303–315 (2007).
7. Dobrovolskaia, M. A., Aggarwal, P., Hall, J. B. & McNeil, S. E. Preclinical studies to understand nanoparticle interaction with the immune system and its potential effects on nanoparticle biodistribution. *Mol. Pharm.* **5,** 487–495 (2008).
8. Linse, S. *et al.* Nucleation of protein fibrillation by nanoparticles. *Proc. Natl Acad. Sci. USA* **104,** 8691–8696 (2007).
9. Reddy, S. T. *et al.* Exploiting lymphatic transport and complement activation in nanoparticle vaccines. *Nature Biotechnol.* **25,** 1159–1164 (2007).
10. Liang, M. *et al.* Cellular uptake of highly packed polymer coated gold nanoparticles. *ACS Nano* **4,** 403–413 (2010).
11. Hall, C. E. & Slayter, H. S. The fibrinogen molecule: its size, shape, and mode of polymerization. *J. Biophys. Biochem. Cytol.* **5,** 11–16 (1959).
12. Lin, Y., Wang, J., Wan, L. J. & Fang, X. H. Study of fibrinogen adsorption on self-assembled monolayers on Au(111) by atomic force microscopy. *Ultramicroscopy* **105,** 129–136 (2005).
13. Lishko, V. K., Kudryk, B., Yakubenko, V. P., Yee, V. C. & Ugarova, T. P. Regulated unmasking of the cryptic binding site for integrin $\alpha_M\beta_2$ in the γ C-domain of fibrinogen. *Biochemistry* **41,** 12942–12951 (2002).
14. Ugarova, T. P. *et al.* Identification of a novel recognition sequence for integrin $\alpha_M\beta_2$ within the γ-chain of fibrinogen. *J. Biol. Chem.* **273,** 22519–22527 (1998).
15. Lishko, V. K., *et al.* Multiple binding sites in fibrinogen for integrin $\alpha_M\beta_2$ (Mac-1). *J. Biol. Chem.* **279,** 44897–44906 (2004).
16. Pasparakis, M. Regulation of tissue homeostasis by NF-κB signalling: implications for inflammatory diseases. *Nat. Rev. Immunol.* **9,** 778–788 (2009).
17. Sitrin, R. G., Pan, P. M., Srikanth, S. & Todd, R. F. 3rd. Fibrinogen activates NF-κB transcription factors in mononuclear phagocytes. *J. Immunol.* **161,** 1462–1470 (1998).
18. Masamune, A. *et al.* Fibrinogen induces cytokine and collagen production in pancreatic stellate cells. *Gut* **58,** 550–559 (2009).
19. Li, Q. & Verma, I. M. NF-κB regulation in the immune system. *Nat. Rev. Immunol.* **2,** 725–734 (2002).
20. Teichroeb, J. H., Forrest, J. A. & Jones, L. W. Size-dependent denaturing kinetics of bovine serum albumin adsorbed onto gold nanospheres. *Eur. Phys. J. E* **26,** 411–415 (2008).
21. Shang, W., Nuffer, J. H., Dordick, J. S. & Siegel, R. W. Unfolding of ribonuclease A on silica nanoparticle surfaces. *Nano Lett.* **7,** 1991–1995 (2007).
22. Lundqvist, M., Sethson, I. & Jonsson, B. H. Protein adsorption onto silica nanoparticles: conformational changes depend on the particles' curvature and the protein stability. *Langmuir* **20,** 10639–10647 (2004).
23. Kim, B. *et al.* Tuning payload delivery in tumour cylindroids using gold nanoparticles. *Nature Nanotech.* **5,** 465–472 (2010).
24. Park, E. J. & Park, K. Oxidative stress and pro-inflammatory responses induced by silica nanoparticles *in vivo* and *in vitro*. *Toxicol. Lett.* **184,** 18–25 (2009).
25. Xia, T. *et al.* Comparison of the abilities of ambient and manufactured nanoparticles to induce cellular toxicity according to an oxidative stress paradigm. *Nano Lett.* **6,** 1794–1807 (2006).
26. Yang, H., Liu, C., Yang, D., Zhang, H. & Xi, Z. Comparative study of cytotoxicity, oxidative stress and genotoxicity induced by four typical nanomaterials: the role of particle size, shape and composition. *J. Appl. Toxicol.* **29,** 69–78 (2009).
27. Diaz, B. *et al.* Assessing methods for blood cell cytotoxic responses to inorganic nanoparticles and nanoparticle aggregates. *Small* **4,** 2025–2034 (2008).
28. Lu, S. *et al.* Efficacy of simple short-term *in vitro* assays for predicting the potential of metal oxide nanoparticles to cause pulmonary inflammation. *Environ. Health Perspect.* **117,** 241–247 (2009).
29. Flick, M. J. *et al.* Leukocyte engagement of fibrin(ogen) via the integrin receptor $\alpha_M\beta_2$/Mac-1 is critical for host inflammatory response *in vivo*. *J. Clin. Invest.* **113,** 1596–1606 (2004).
30. Ryu, J. K. & McLarnon, J. G. A leaky blood–brain barrier, fibrinogen infiltration and microglial reactivity in inflamed Alzheimer's disease brain. *J. Cell. Mol. Med.* **13,** 2911–2925 (2008).
31. Butcher, N. J. & Minchin, R. F. Arylamine *N*-acetyltransferase 1 gene regulation by androgens requires a conserved heat shock element for heat shock factor-1. *Carcinogenesis* **31,** 820–826 (2010).

Acknowledgements

This work was supported by grants from the Australian Research Council (DP8787331) and the National Health and Medical Research Council (569694).

Author contributions

Z.J.D. performed all the biological experiments, assisted in designing the biological experiments and co-wrote the manuscript. M.L. synthesized and characterized the nanoparticles. M.M. and I.T. designed the nanoparticle synthesis procedure. R.F.M. conceived and designed the biological studies and co-wrote the manuscript.

Additional information

The authors declare no competing financial interests. Supplementary information accompanies this paper at www.nature.com/naturenanotechnology. Reprints and permission information is available online at http://npg.nature.com/reprintsandpermissions/. Correspondence and requests for materials should be addressed to R.F.M.